Journal of Fluorescence (2019) 29:155–163
https://doi.org/10.1007/s10895-018-2323-3

ORIGINAL ARTICLE

Development of a Highly Selective Two-Photon Probe for Methylglyoxal and its Applications in Living Cells, Tissues, and Zebrafish

Shiying Gao[1] · Yonghe Tang[1] · Weiying Lin[1]

Received: 16 August 2018 / Accepted: 5 November 2018 / Published online: 12 November 2018

Abstract

Methylglyoxal (MGO) is one of the most important active carbonyl compounds in living organisms. It is a metabolic by product of glycolysis. MGO participates in glycosylation of proteins and nucleic acids to trigger carbonyl stress, inducing pathological status and even exacerbateing the development of chronic degenerative diseases. In order to study the diseases caused by MGO, it is meaningful for us to develop methods that could efficiently detect MGO. In our work, a new two-photon fluorescent turn-on probe which named **NP** has been designed which was made up of naphthalimides dye as the two-photon fluorescent platform and the *o*-phenylenediamine as recognition site. When reacted with MGO, **NP** showed excellent sensitivity and selectivity. Based on the two-photon fluorescence imaging technology, **NP** has firstly successful application in living cells, tissues and zebrafish to detecting MGO.

Keywords Fluorescence probe · Methylglyoxal · Two-photon · Turn-on · Naphthalimides dye

Introduction

Methylglyoxal (MGO), also known as pyruvaldehyde, is an important bioactive carbonyl compound. MGO can be produced gradually in the process of food production and storage. In addition, higher concentrations of MGO were detected in milk, coffee, cola and other beverages [1]. The endogenous MGO is mainly comes from the by-products of glycolysis through oxidative metabolism [2–5]. For example, endogenous MGO is produced by propionic phosphate, including dihydroxyacetone phosphate and glyceraldehyde triphosphate, catalyzed by the propionic phosphatase and methyl ethylaldehyde synthase [6, 7]. The processes of lipid and acetone peroxidation, amino acid degradation, and Amadori rearrangement can also produce endogenous MGO [8, 9]. MGO has high reactivity and is easy to react with the biomolecules containing amino or mercapto groups to form glycosylated compounds [10]. Medical research shows that MGO is directly related to diabetes, alzheimer's disease, cardiovascular disease and other diseases [7]. Therefore, it is of great significance to developing effective methods for the detection of MGO and it is the basis of learning its toxicity to disease research.

Currently, the fluorescence imaging technology is a promising method to detect biologically active molecules in living systems due to the non-destructive detection, high selectivity and sensitivity [11–15]. To data, several MGO fluorescent probes have been reported [16–18]. However, they generally utilize one-photon (OP) light and provide short emission wavelength fluorescent signal output (less than 600 nm). By contrast, the two-photon (TP) imaging microscopy technology usually employed near-infrared excitation source (more than 600 nm), and exhibited some advantages, including the less photo-damage, deep penetration, three-dimensional (3D) imaging, and less auto-fluorescence interference [18]. Accordingly, it's urgent to develop a two-photon fluorescence probe which can be utilized to detecting the MGO in biological systems.

Herein, we presented a new two-photon fluorescent probe **NP** for detecting of MGO. The **NP** contained the two-photon fluorescent platform of naphthalimides dye, and the recognition site of *o*-phenylenediamine. With the introduction of MGO, **NP** can give out significant fluorescence enhancement signal at about 555 nm. **NP** showed excellent sensitivity and selectivity to MGO. What's more, **NP** has been propitious utilized in the two-photon imaging of the MGO in cells, tissues and zebrafish.

Electronic supplementary material The online version of this article (https://doi.org/10.1007/s10895-018-2323-3) contains supplementary material, which is available to authorized users.

✉ Weiying Lin
weiyinglin2013@163.com

[1] Institute of Fluorescent Probes for Biological Imaging, School of Chemistry and Chemical Engineering, School of Materials Science and Engineering, University of Jinan, Shandong 250022, People's Republic of China

Experimental

Materials and Instruments

All raw materials and reagents from supplier were directly used without further purification. 3-Methoxyaniline was purchased from *Tianjin Heowns Biochemical Technology Co., Ltd.*, 1-bromo-3-chloropropane was purchased from *J&K Scientific Ltd.*, hydriodic acid (HI) was purchased from *Zhengzhou Alfachem Co.,Ltd.* The hydrazine was dissolved into ultrapure water. Absorption spectra were tested by a UV-vis spectrophotometer (Shimadzu UV-2600, Japan). Fluorescent spectra were tested by a fluorescence spectrophotometer (HITACHI F4600, Japan). The pH measurements were performanced on a pH meter (Mettler-Toledo Delta 320, Switzerland). High-resolution mass spectra (HRMS) were recorded on a mass spectrometer (Bruker Apex Ultra 7.0 T FTMS, Germany) in electrospray ionization (ESI) mode. NMR spectra were recorded on a 400 MHz Digital NMR Spectrometer (Bruker AVANCE III, Germany), using tetramethylsilane (TMS) as internal reference.

The NP Synthesis Steps

The routes of compound **1**, **2** and **NP** synthesis was shown in Scheme 1.

The Synthesis of Compound 1

4-bromo-1,8-naphthalic anhydride (554 mg, 2 mmol) and 2-nitrobenzene-1,4- diamine (306 mg, 2 mmol) were dissolved in 20 mL ethanol, refluxed for 5–6 h. After the solution gradually deepened from the pale yellow to dark brown, the whole reaction system was cooled down and gradually deposited with yellow solid. After vacuum filtration, the cake was washed with ice ethanol for 2–3 times. After drying, the compound **1** (774 mg, yield: 91%) was obtained without purification.

The Synthesis of Compound 2

Compound **1** (441 mg, 1 mmol) in 2-methoxyethanol (30 mL) added with n- butylamine (1 mL, 1 mmol) dropwise, refluxed overnight. Then removed solvent under reduced pressure. The crude material was purified by flash chromatography (dichloromethane: methanol = 10:1) to give the compound **2** (382 mg, yield: 77%). ^{1}H NMR (400 MHz, DMSO-d_6) δ 8.76 (d, J = 8.4 Hz, 1H), 8.43 (d, J = 7.6 Hz, 1H), 8.26 (d, J = 8.4 Hz, 1H), 7.95 (d, J = 2.4 Hz, 1H), 7.83 (t, J = 5.6 Hz, 1H), 7.71 (t, J = 8.0 Hz, 1H), 7.62 (s, 2H), 7.36 (dd, J_1 = 8.8 Hz, J_2 = 2.4 Hz, 1H), 7.10 (d, J = 8.8 Hz, 1H), 6.81 (d, J = 8.8 Hz, 1H), 3.40 (q, J = 6.8 Hz, 2H), 1.71 (m, 2H), 1.45 (m, 2H), 0.96 (t, J = 7.2 Hz, 3H); ^{13}C NMR (100 MHz, DMSO-d_6) δ 164.63, 163.70, 151.30, 146.24, 137.47, 134.84, 131.25, 130.37, 130.19, 129.25, 126.16, 124.62, 124.36, 122.68, 120.67, 119.67, 108.09, 104.23, 30.43, 26.80, 20.32, 14.23; HR-MS calculated for $C_{22}H_{20}N_4O_4$ $[M+H]^+$ m/z 405.1557, found $[M+H]^+$ m/z 405.1554(Fig. S1-S3).

The Synthesis of NP

Compound **2** (404 mg, 1 mmol) in ethanol (20 mL) stirred slowly with adding 1 mL containing 5 mmol $SnCl_2$ concentrated hydrochloric acid solution, then refluxed for 3 h. Until the mixture cooled, and the yellow solid would be settled. After vacuum filtration, the cake obtained by ultra-pure water washing to neutral. The crude product was purified by flash chromatography (dichloromethane: methanol = 10:1) to get the probe **NP** (248 mg, yield: 67%). ^{1}H NMR (400 MHz, DMSO-d_6) δ 8.75 (d, J = 8.4 Hz, 1H), 8.41 (d, J = 7.2 Hz, 1H), 8.24 (d, J = 8.4 Hz, 1H), 7.82 (t, J = 5.6 Hz, 1H), 7.70 (t, J = 7.6 Hz, 1H), 6.83 (m, 2H), 6.64 (s, 1H), 6.63 (s, 4H), 6.54 (d, J = 8.0 Hz, 1H), 3.39 (q, J = 6.8 Hz, 4H), 1.71 (m, 2H), 1.44 (m, 2H), 0.96 (t, J = 7.2 Hz); ^{13}C NMR (100 MHz, DMSO-d_6) δ 164.60, 163.75, 151.26, 134.86, 134.85, 131.28, 130.28, 129.19, 124.75, 122.63, 122.61, 121.77, 121.63, 120.62, 119.24, 119.10, 108.04, 104.29, 43.02, 30.38, 20.27, 14.22; HR-MS calculated for $C_{22}H_{22}N_4O_2$ $[M+H]^+$ m/z 375.1816, found $[M+H]^+$ m/z 375.1813(Fig. S4-S6).

Preparation for the Spectroscopic Test

All the spectrum measurements were carried out as following. The stock solution of **NP** was prepared in DMSO and the

Scheme 1 Synthesis route of the **NP**

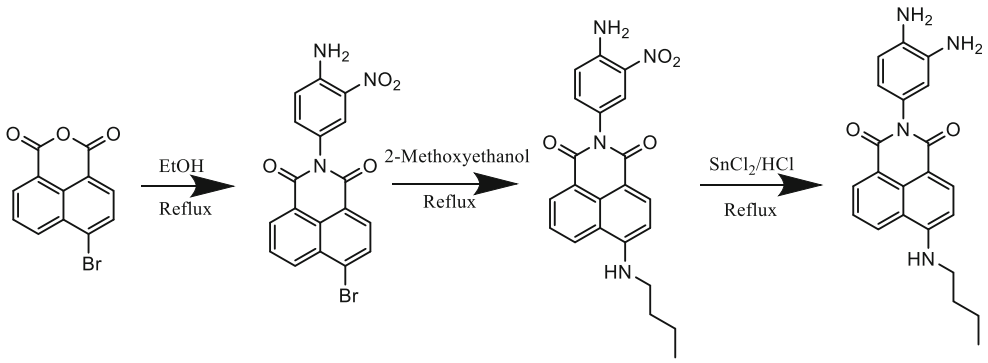

concentration was 1.0 mM. MGO was dissolved in ultrapure water to get the test storage solution with a concentration of 10 mM. Other analytes (cationic/anionic) were also prepared with ultrapure water as test storage solutions with a concentration of 10 mM.

Before the spectrum test, 25 μL probe **NP** test storage solution and 250 μL DMSO were placed in the 5 mL volumetric flask, then used 10 mM PBS buffer to adjust the final volume to 5 mL to get test probe solution.

For the fluorescent titration test, different concentrations of MGO test storage solution were added to the test probe solution and recorded after 60 min of incubation.

For the pH study, 25 μL **NP** test storage solution and 250 μL DMSO were placed in the 5 mL volumetric flask, then used 10 mM PBS buffer (different pH value) to adjust the final volume to 5 mL to get pH test probe solution. Then added 10 μL MGO test storage solution to the above pH test probe solution, then recorded after 60 min of incubation.

For the selective spectrum test, requisite amount of analytes test storage solutions was added to the above test probe solutions, and then incubated for 60 min at room temperature.

DFT Calculations

The theoretical calculations were performed by the software of Gaussian 09. The orbital energy of excited dye and recognition sites (before and after reacted with MGO) were performed by using DFT with B3LYP functional and 6-31G basis set. The initial geometric shapes of excited dye and recognition sites (before and after reacted with MGO) were generated by the software of GaussView.

Cell Culture and Bio-Imaging

HeLa cells were cultured in Dulbecco's modified eagle medium (DMEM) supplemented with 10% FBS (fetal bovine serum) and incubated at 37 °C in air atmosphere (5% CO_2).

t?>Before the imaging experiments, Hela cells were seeded in confocal plates (2×10^4 cells/mL). After 24 h, in the control group, the cells were pretreated with 5 μM **NP** for 60 min at 37 °C. Cell imaging was performed after the cells were washed twice with PBS. In the imaging of exogenous MGO, Hela cells were pretreated with MGO (100 μM) for 60 min and washed three times with PBS. Then Hela cells were treated with **NP** (5 μM) for 60 min, washed three times with PBS. The one-photon fluorescence excited at 488 nm for the green channel (500–550 nm). The two-photon fluorescence excited at 760 nm.

Liver Tissue Bio-Imaging Using MGO

Rat brain slices were prepared from the liver of 4-weeks-old living Balb/c mice, which was approved by the Animal Ethical Experimentation Committee of Shandong University. The fresh brain tissues were incubated with 5 μM probe **NP** for 60 min, and then, 100 μM MGO was added for another 60 min. Before imaging, the tissues were washed with PBS three times. A Nikon A1R confocal microscope with a 40 × objective lens was used for fluorescence images. All of these experiments meet the relevant laws and institutional guidelines.

Zebrafish Bio-Imaging Using MGO

Wild type zebrafishes were obtained from the Nanjing Ezerinka Biotechnology Co., Ltd. 3-day-old zebrafishes were transferred into confocal plates, and 5 μM probe **NP** was fed for 60 min; then, 100 μM MGO was added and further incubated for another 60 min. After that, the zebrafishes were transferred

Scheme 2 Reaction mechanism of the **NP**

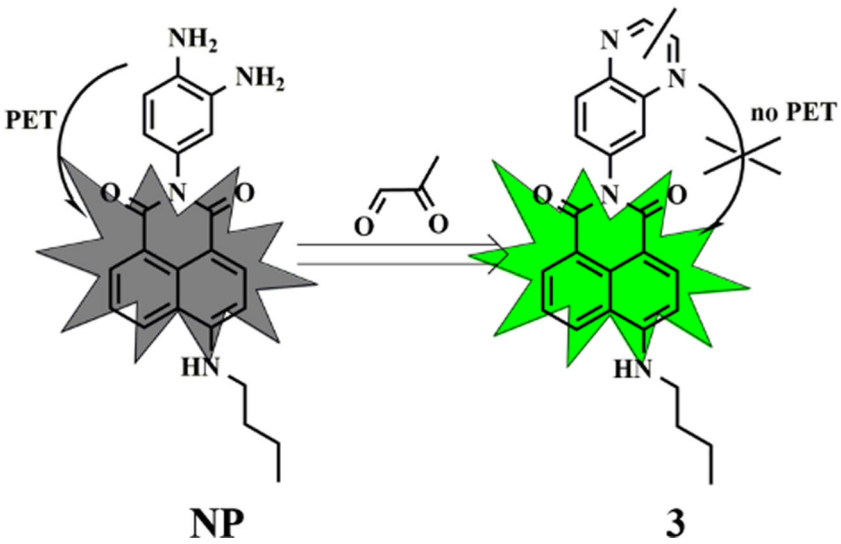

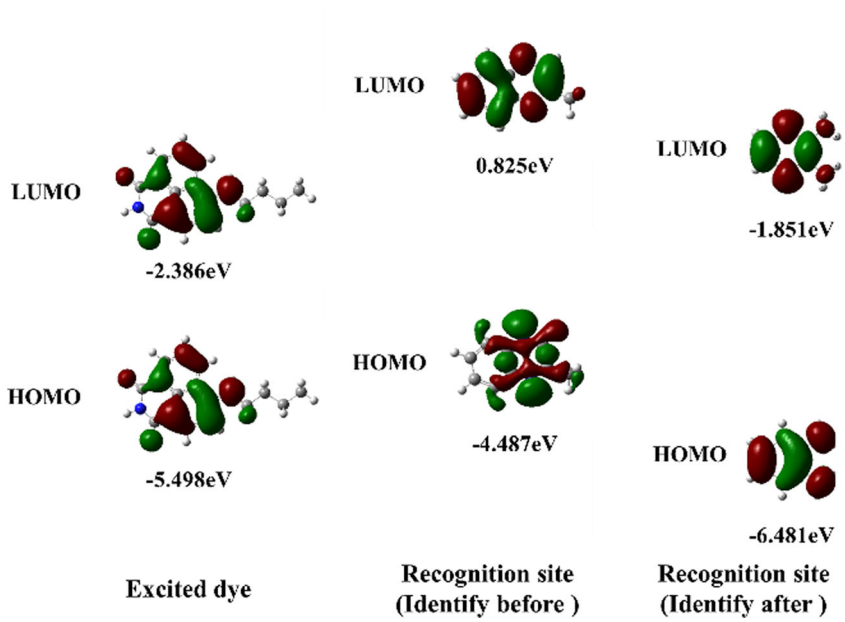

Fig. 1 Molecular orbital plots (LUMO and HOMO) and HOMO/LUMO energy gaps of **NP**. In the ball-and-stick representation, hydrogen, carbon, nitrogen and oxygen are colored in light gray, gray, blue, red, and pink, respectively

into new glass bottom dishes for imaging. Fluorescence images were acquired with a Nikon A1R confocal microscope with a 4× objective lens. The excitation and emission wavelengths were the same as for fluorescence imaging in living cells.

Results and Discussion

Design and Synthesis of the NP

Naphthalimides dyes have many significant features, including excellent two-photon properties, excellent optical stability, and high fluorescence quantum yield, so the naphthalimides dyes are widely used in the fluorescence probe design [19–28]. Because of the PET (Photoinduced Electron Transfer) effect caused by the *o*-phenylenediamine group, the probe showed non-fluorescent. With the introduction of MGO, there is no existence of the PET effect because of the condensation-cyclization reaction between *o*-phenylenediamine group and MGO. At the same time, the fluorescent intensity of **NP** showed significant enhancement (Scheme 2). This hypothesis was supported by the theoretical calculations (Fig. 1). The structure of **NP** was confirmed by ^{1}H NMR, ^{13}C NMR, and HR-MS.

Spectral Response of Probe towards MGO

The fluorescent spectra of **NP** for MGO were investigated. As shown in Fig. 2a, only **NP** which was excited with 440 nm showed weak fluorescence in 555 nm because of the effect of PET. After the introduction of MGO, a distinct fluorescence peak was observed with the equivalent concentration increased of MGO, and the

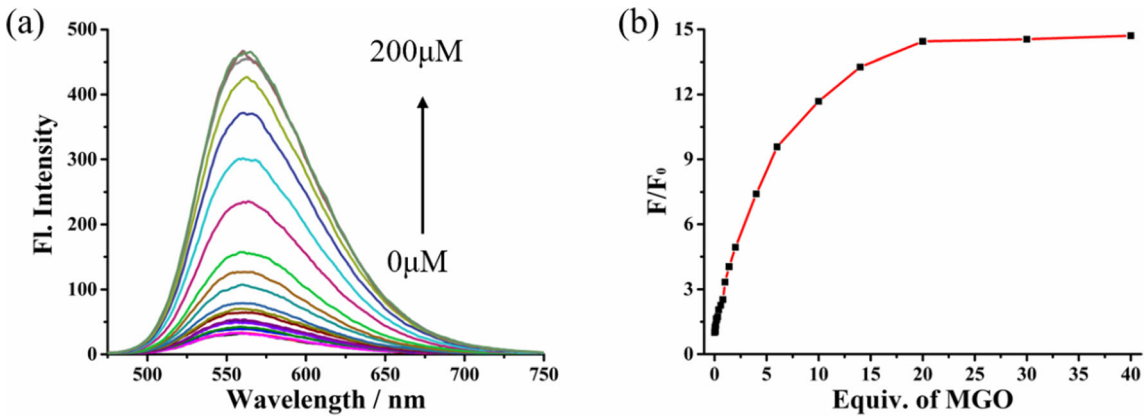

Fig. 2 **a** The fluorescence titration curve of the interaction between 5 μM **NP** and different concentrations of MGO (0–200 μM solution); **b** The change curve of the fluorescence intensity enhancement with equivalent change of the MGO and **NP** in the DMSO/PBS buffer (pH = 7.4, *v*/v = 1:19) λ_{ex} = 440 nm

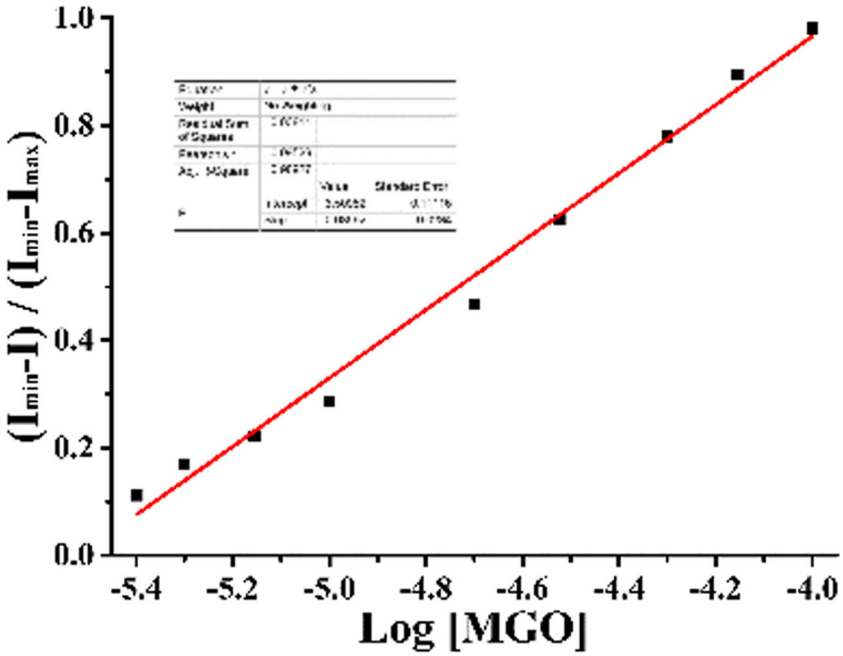

Fig. 3 Normalized variation of fluorescence signal with the changing concentration of MGO

intensity of fluorescence at 555 nm reached the maximum in the presence of 150 μM MGO (Fig. 2b). At the same time, an effective linear relation between the intensity of fluorescence at 555 nm and MGO level ranging from 0 μM to 6 μM could be obtained, and the low detection limit was calculated to 1.47 μM referred to Fig. 3. It is noteworthy that the low detection limit of **NP** may make it very desirable to observe the level of MGO in vivo.

Subsequently, dynamic tests of NP towards MGO were evaluated. After the treatment of 5 μM **NP** with 0 μM, 100 μM and 150 μM MGO, the fluorescence intensity at 555 nm grew with time (Fig. 4). The equilibrium state achieved of **NP** (5 μM) treated with MGO (150 μM) about 40 min. Under the pseudo-first-order conditions, the rate constant for the probe was determined to be $k = 0.07\ min^{-1}$ (Fig. 4b). Therefore, **NP** can be served as a sensitive probe for MGO and may help to detect the changes of MGO in bio-systems.

Recognition Mechanism of Probe towards MGO

The recognition mechanism of **NP** to MGO was investigated by the MS assay. After the treatment of **NP** with MGO in 10 mM PBS (pH 7.4), the MS data (Fig. S8) showed that a peak at 411.2 corresponding to compound **3** (calculated for $[M + H]^+$ m/z 411.2) could be observed clearly. It confirms

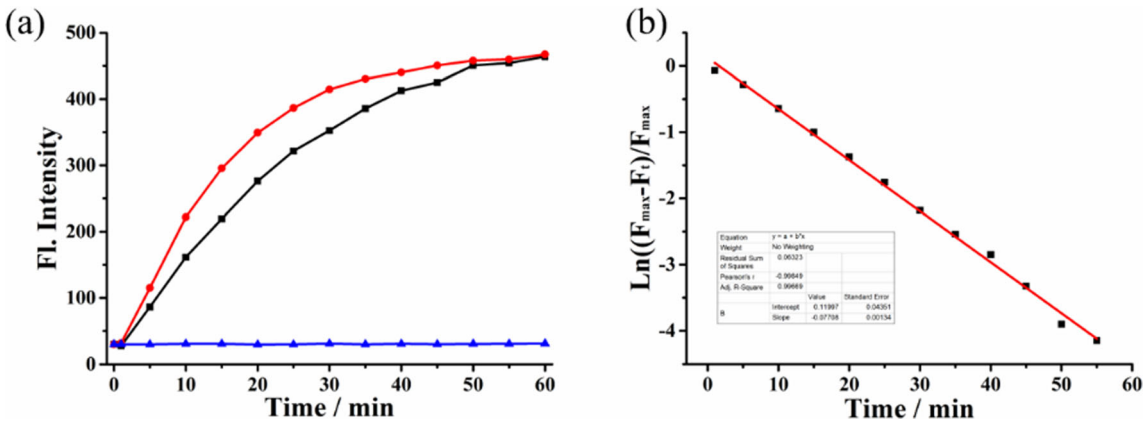

Fig. 4 **a** Kinetic studies curve of **NP** (5 μM) treated with MGO (0,100 and 150 μM) in the DMSO/ PBS buffer (pH = 7.4, v/v = 1:19). $\lambda_{ex} = 440$ nm; **b** *Pseudo*-first-order kinetic plot of the reaction of **NP** (5 μM) with MGO (150 μM) in the DMSO/ PBS buffer (pH = 7.4, v/v = 1:19). Slope = 0.07 min^{-1}

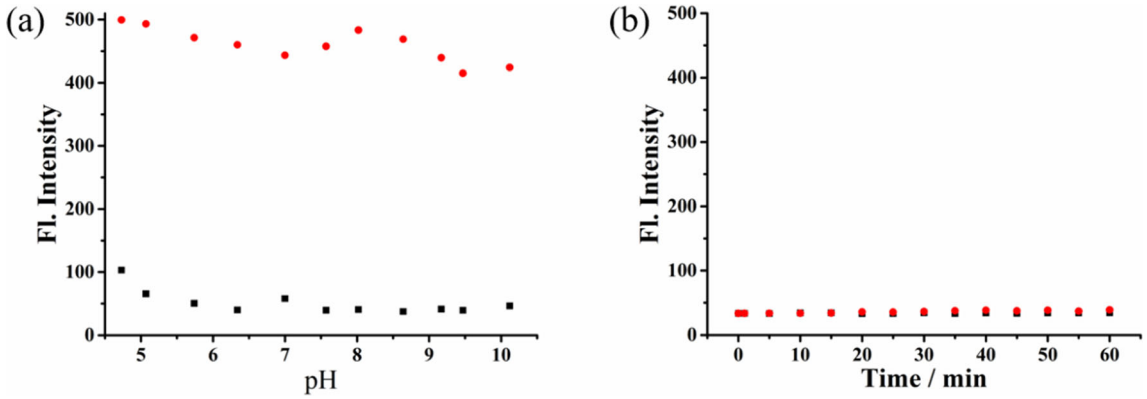

Fig. 5 **a** Fluorescence intensity of free sensor **NP** (5 μM) [■] and in the presence of 150 μM MGO [■] with different pH; **b** Photostability profiles of **NP** (5 μM) in the absence or presence of UV-irradiated (365 nm). The fluorescence intensities were continuously monitored at time [■]light; [■] unlight

that **NP** undergoes the condensation-cyclization reaction with MGO to provide the compound **3**.

The Effect of pH, Selectivity and Photo-Stability Studies

The pH of the test solution (or cellular microenvironment) may affected the ability of the probe to recognize MGO. Then we carried out the pH effect tests about **NP** in the absence or presence of MGO. In the pH range of the test, the fluorescence intensity of **NP** was almost invariable. At the same time when MGO was added, the fluorescence signal fluctuated slightly in the range of 4.5–10.0 (Fig. 5a). The experimental data indicated the potential applications of the probe in biological samples at physiological pH environment. After that, the stability of **NP** was detected, and the results indicated that **NP** has excellent photo-stability (Fig. 5b). The selectivity of **NP** to MGO was evaluated by the determination of its fluorescence spectra treated with a variety of biologically relevant species. As shown in the Fig. 6, only MGO could make significant change in fluorescence intensity at 555 nm, whereas the other relevant analytes showed almost no change in fluorescence intensity. Although the *o*-phenylenediamine group is also the recognition site for nitric oxide (NO), with the introduction of NO only slightly fluorescence changes (about 1.6-fold) was obtained during the same incubating time. These results indicated that **NP** is highly sensitive to MGO over other analytes.

Cell Imaging of NP towards MGO

We had taken MTT assay to determined cell viability before the imaging experiment. The viability was more than 80% when the HeLa cells were incubated with **NP** (0–40 μM) for 24 h, meaning that **NP** has low cytotoxicity and can be used for cell imaging (Fig. S7).

The utility of probe **NP** for imaging of MGO in living cells was investigated under OP and TP modes. As shown in Fig.7e-h, the HeLa cells incubated with only the probe **NP** displayed almost no fluorescence. In contract, when incubated with 5 μM probe **NP** for 60 min and then treated with 100 μM MGO for another 60 min, the HeLa cells exhibited enhanced fluorescence in the green channel at the OP mode. (Fig.7i-k). Meanwhile, the obvious (Fig.7l) green fluorescence increase can also be noted at the TP mode. These studies showed that

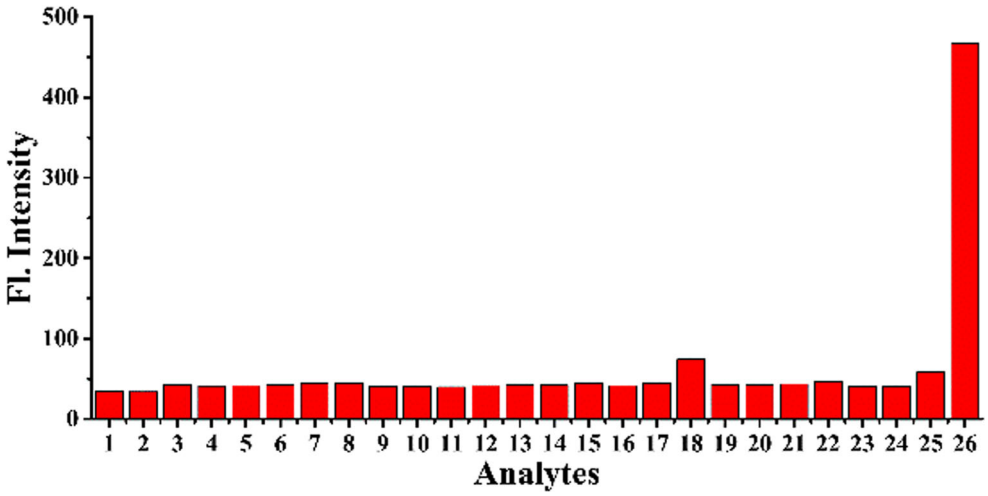

Fig. 6 The fluorescence intensity of **NP** (5 μM) in the presence of 150 μM MGO in the DMSO/PBS buffer (pH = 7.4, v/v = 1:19) and 200 μM ions, anions and ROS; The analytes were in turn: 1: only the probe; 2: Cu^{2+}; 3: Mg^{2+}; 4: NO_3^-; 5: NO_2^-; 6: HSO_3^-; 7: S^{2-}; 8:SO_4^{2-}; 9: Fe^{2+}; 10: I^-; 11: Br^-; 12: ClO^-; 13: H_2O_2; 14: Thr; 15: Hcy; 16: Cys; 17: GSH; 18: NO; 19: Glu; 20: ONBD; 21: Pyr; 22: FA; 23: Alk; 24: Tri; 25: Gly; 26: MGO

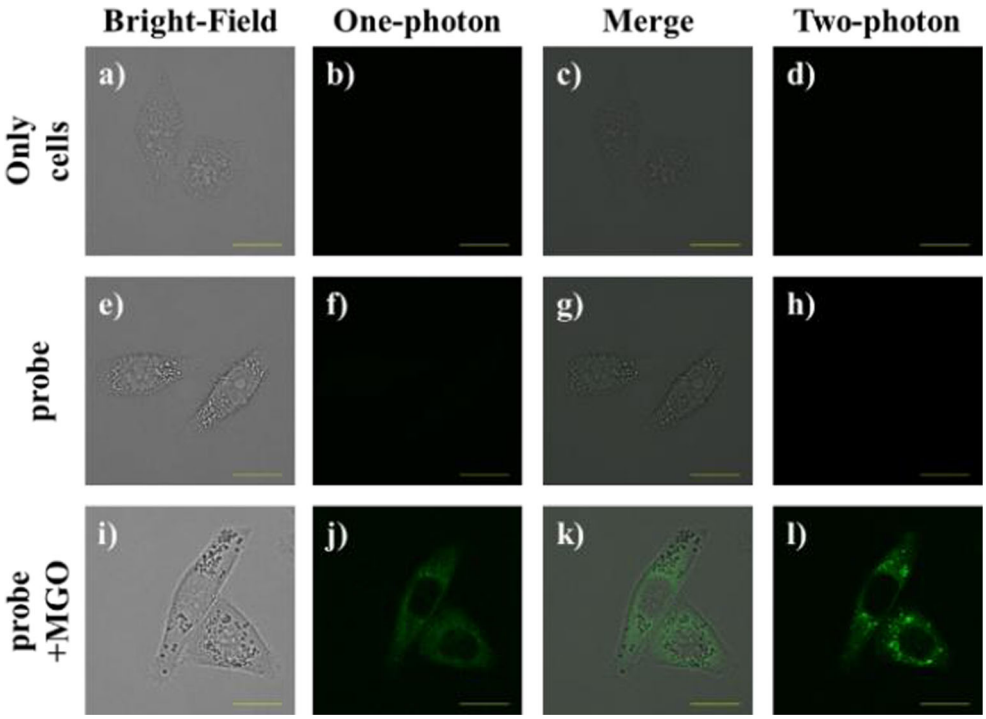

Fig. 7 The fluorescence imaging of **NP** in Hela cells. **a**-**d**) The imaging for the HeLa cells; **e**-**h**) The imaging for the HeLa cells treated with **NP** (5 μM). **i**-**l**) The imaging for the HeLa cells treated with MGO (100 μM) and **NP** (5 μM). The cells were excited at 488 nm, and the emission collection was from 500 to 550 nm. Scale bar: 20 μm

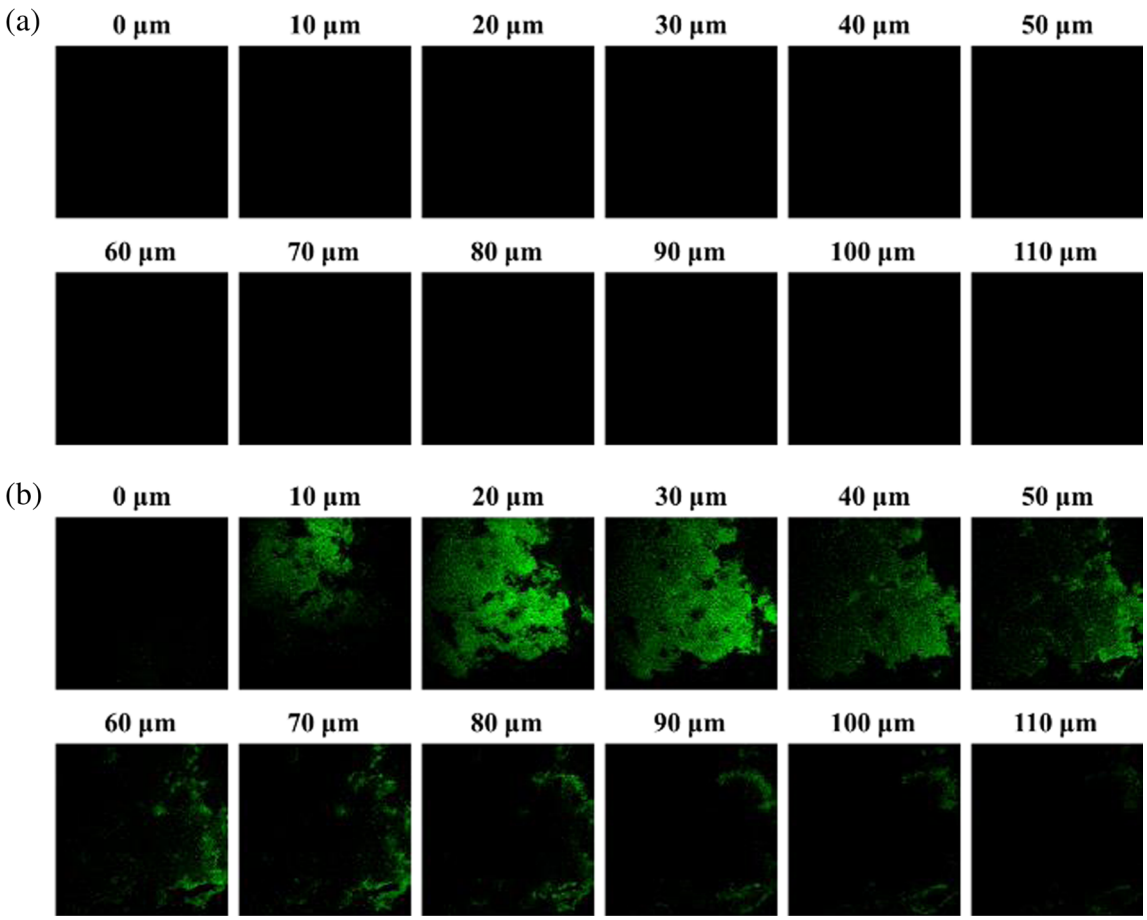

Fig. 8 The fluorescence imaging of **NP** in liver tissues. **a** Tissue slices only treated with **NP** (30 μM);(**b**) tissue slices added **NP** (30 μM) in present of MGO (200 μM). The liver slides were excited at 760 nm. And the emission collection was from 500 to 550 nm

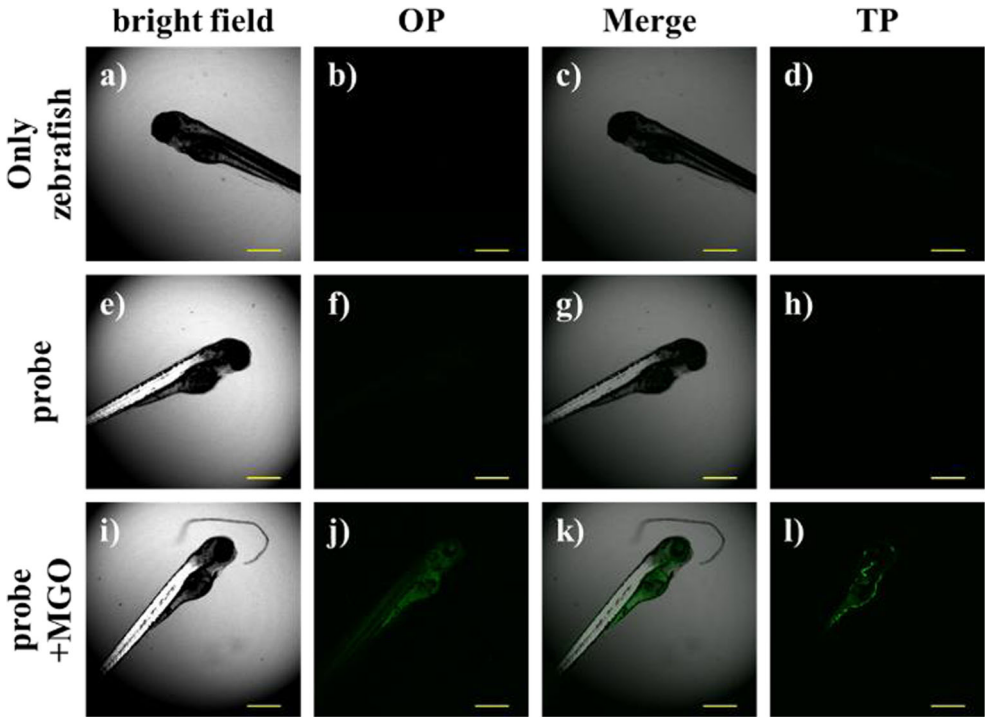

Fig. 9 Fluorescence images of zebrafish at one-photon and two-photon modes. **a**-**d**) are the blank group. **e** − **h**) are the fluorescence images of zebrafish treated with 10 μM **NP**. **i** − **l**) are the fluorescence images of zebrafish treated with 100 μM MGO and then treated with 10 μM **NP**. Scale bar: 500 μm

NP has a good membrane permeability and can be applied for monitoring exogenous MGO in living cells.

Liver Tissue Imaging of NP towards MGO

Encouraged by cells imaging applications of **NP** with MGO, then we applied **NP** to image MGO in living liver tissue slices. As a control group, the living tissues only loaded **NP** displayed weak fluorescence (Fig. 8a). After the further incubation with MGO for another 60 min, the living tissues exhibited strong green fluorescence (Fig. 8b). It can be observed that the penetration depth could approximate 110 μm. These data indicated that the probe **NP** can be applied for the visualization of MGO in living tissues.

Zebrafish Imaging of NP towards MGO

Finally, we proceeded to test the ability of **NP** to visualize MGO in living zebrafish. As shown in Fig.9e-h, the the living zebrafish incubated with only the probe **NP** exhibited weak fluorescence. In comparison, when incubated with the probe **NP** and MGO, the zebrafish displayed enhanced fluorescence under OP excitation. (Fig.7i-l). Notably, the same fluorescence changes were also obtained (Fig.7l) under TP excitation. These studies showed that **NP** could enter zebrafish and detect MGO in living zebrafish under OP and TP modes.

Conclusion

In conclusion, a new two-photon fluorescent turn-on probe **NP** which was combined with naphthalimides dye as fluorophore platform and *o*-phenylenediamine as the MGO recognition site. **NP** had almost no fluorescence due to the PET effect from the *o*-phenylenediamine group to the naphthalimides dye. With the intervention of MGO, the PET effect was broken because of the condensation-cyclization reaction between the group of *o*-phenylenediamine and MGO, showed great enhancement of fluorescence signal. The probe showed the characteristics of highly sensitive and selective responded to MGO. Significantly, **NP** has been propitious applied to the two-photon imaging of MGO in cells, tissues and zebrafish for the first time. All these features showed that the probe **NP** has the potential to practical applications in biological systems.

Acknowledgements This work was financially supported by NSFC (21472067, 21672083, 21877048), Taishan Scholar Foundation (TS 201511041), and the startup fund of the University of Jinan (309-10004).

References

1. Wang J, Chang T (2010) Methylglyoxal content in drinking coffee as a cytotoxic factor. J Food Sci 75(6):H167–H171
2. Phillips SA, Thornalley PJ (1993) The formation of methylglyoxal from triose phosphates. Eur J Biochem 212(1):101–105
3. Rabbani N, Thornalley PJ (2008) Dicarbonyls linked to damage in the powerhouse: glycation of mitochondrial proteins and oxidative stress. Biochem Soc Trans 36(5):1045–1050

4. Thornalley PJ (2008) Protein and nucleotide damage by glyoxal and methylglyoxal in physiological systems - role in ageing and disease. Drug Metabol Drug Interact 23(1):125–150
5. Thornalley PJ (1996) Pharmacology of methylglyoxal: formation, modification of proteins and nucleic acids, and enzymatic detoxification-a role in pathogenesis and antiproliferative chemotherapy. Gen Pharmacol 27(4):565–574
6. Rose IA, Nowick JS (2002) Methylglyoxal synthetase, enol-pyruvaldehyde, glutathione and the glyoxalase system. J Am Chem Soc 124(44):13047–13052
7. Song F, Schmidt AM (2012) Glycation and insulin resistance. Arterioscler Thromb Vasc Biol 32(8):1760–1765
8. Li X-H, Du L-L, Cheng X-S (2013) Glycation exacerbates the neuronal toxicity of β-amyloid. Cell Death Dis 4(6):e673
9. Casazza JP, Felver ME, Veech RL (1982) The metabolism of acetone in rat. J Biol Chem 259(1):231–236
10. Yan SJ, Wang L, Li Z (2012) Inhibition of advanced glycation end product formation by Pu-erh tea ameliorates progression of experimental diabetic nephropathy. J Agric Food Chem 60(16):4102–4110
11. Chen H, Dong B, Tang Y, Lin W (2017) A unique "integration" strategy for the rational design of optically tunable near-infrared fluorophores. Acc Chem Res 50(6):1410–1422
12. Cao L, Zhang R, Zhang W (2015) A ruthenium (II) complex-based lysosome-targetable multisignal chemosensor for in vivo detection of hypochlorous acid. Biomaterials 68:21–31
13. Zhang F, Liang X, Zhang W (2016) A unique iridium (III) complex-based chemosensor for multi-signal detection and multi-channel imaging of hypochlorous acid in liver injury. Biosens Bioelectron 87:1005–1011
14. Yuan L, Lin W, Feng Y (2011) A rational approach to tuning the pKa values of rhodamines for living cell fluorescence imaging. Org Biomol Chem 9(6):1723–1726
15. Guan X, Lin W, Huang W (2014) Development of a new rhodamine-based fret platform and its application as a Cu^{2+} probe. Org Biomol Chem. 12(23):3944–3949
16. Zhang W, Zhang F, Wang YL, Song B, Zhang R, Yuan J (2017) Red-emitting ruthenium(ii) and iridium(iii) complexes as phosphorescent probes for methylglyoxal in vitro and in vivo. Inorg Chem 56(3):1309–1318
17. Wang T, Douglass EF Jr, Fitzgerald KJ, Spiegel DA (2013) A "turn-on" fluorescent sensor for methylglyoxal. J Am Chem Soc 135(33):12429–12433
18. Liu S, Luo Y, Liang G (2015) In situ clicking methylglyoxal for hierarchical self-assembly of nanotubes in supramolecular hydrogel. Nanoscale 8(2):766–771
19. Xie XL, Tang FY, Shangguan XY (2017) Two-photon imaging of formaldehyde in live cells and animals utilizing a lysosome-targetable and acidic pH-activatable fluorescent probe. Chem Commun 53(48):6520–6523
20. Xie ZD, Ge JY, Zhang HT (2017) A highly selective two-photon fluorogenic probe for formaldehyde and its bioimaging application in cells and zebrafish. Sensors Actuators B Chem 241:1050–1056
21. Liu C, Cheng AW, Xia XK (2016) Development of a facile and sensitive fluorimetric derivatization reagent for detecting formaldehyde. Anal Methods 8(13):2764–2770
22. Bi AY, Gao T, Cao XZ (2018) A novel naphthalimide-based probe for ultrafast, highly selective and sensitive detection of formaldehyde. Sensors Actuators B Chem 255:3292–3297
23. Chen J, Zeng LY, Xia T (2015) Toward a biomarker of oxidative stress: a fluorescent probe for exogenous and endogenous malondialdehyde in living cells. Anal Chem 87(6):8052–8056
24. Lee MH, Han JH, Lee JH (2012) Mitochondrial thioredoxin-responding off-on fluorescent probe. J Am Chem Soc 134(41):17314–17319
25. Fan J, Han Z, Kang Y (2016) A two-photon fluorescent probe for lysosomal thiols in live cells and tissues. Sci Rep 6:19562–19565
26. Sun YQ, Wang P, Liu J (2012) A fluorescent turn-on probe for bisulfite based on hydrogen bond-inhibited C=N isomerization mechanism. Analyst 137(15):3430–3433
27. He L, Lin W, Xu Q (2015) A new strategy to construct a FRET platform for ratiometric sensing of hydrogen sulfide. Chem Commun 51(8):1510–1513
28. Feng W, Mao Z, Liu L (2017) A ratiometric two-photon fluorescent probe for imaging hydrogen sulfide in lysosomes. Talanta 167:134–142